# Growth Kinetics of Ultrathin Silicon Dioxide Films Formed by Rapid Thermal Oxidation

Hisashi FUKUDA, Katsunori AKASE, Toshiaki ENDOH and Shigeru NOMURA

*Department of Electrical and Electronic Engineering, Faculty of Engineering,*

*Muroran Institute of Technology*

*27-1 Mizumoto, Muroran, Hokkaido 050, Japan*

We have proposed a practical model for ultrathin (<10 nm) $SiO_2$ film growth in rapid thermal oxidation (RTO) kinetics. The results showed that the overall RTO growth can be well described by the linear-parabolic model proposed by Deal and Grove. Moreover, the model proposed indicates that in order to fit the experimental data, the oxide growth in a ramp-up process must be included in the linear-parabolic scheme. As a result, we have succeeded in explaining the RTO growth kinetics in the RTO range from 950 to 1200 °C and in a wide thickness range from 1.5 to 25 nm without making any special assumptions.

## 1. INTRODUCTION

Owing to continuing demands for the scaling down of ULSIs, demonstration of the integrity and high reliability of ultrathin (<10 nm) $SiO_2$ film is urgently required. In fact, it is expected that the oxide thickness must be decreased from 20 nm for 1.25-µm CMOSFETs to 7 nm for 0.25 µm ULSI devices owing to downscaling of devices.[1] Hitherto, ultrathin $SiO_2$ films have usually been formed in diluted oxidant gas and by lowering the growth temperature in a furnace tube.[2,3] However, it has been reported that oxide films grown by these oxidation processes result in inferior $SiO_2/Si$ interface characteristics in terms of electrical properties, for example, high density of interface trap states, high oxide trap density, and low oxide breakdown fields.[4] Recently, rapid thermal oxidation (RTO) has been proposed for ultrathin $SiO_2$ film formation.[5,6] One of the advantages is that, owing to high-temperature ( >1000°C ) processing, the RTO films show superior oxide quality in the oxide charge and excellent oxide breakdown characteristics as compared to those of conventional furnace oxidation. In addition, the control of oxide thickness is much easier to achieve in RTO than in conventional oxidation. Moreover, RTO provides the possibility of minimizing the thermal budget (time/temperature product), which is necessary for future ULSI fabrication.[7] Recently, demands have been increased for the precise control of oxide thickness as well as for thickness uniformity at the wafer level. In fact, accuracy on the order of 0.1 nm is required for ultrathin oxide formation. To this end, the simulation of the oxide thickness becomes more important. However, very little attention has been focused on the oxidation kinetics.

In this paper, we propose a practical model to explain the RTO kinetics over a wide temperature range from 950 to 1200 °C .

## 2. EXPERIMENTAL

The starting materials were B-doped Czochralski (CZ)-grown (100), (111) and (110) silicon wafers with 125-mm diameter. The RTO apparatus consists of arrayed tungsten-halogen lamps as the heating source, and an optical pyrometer to measure and to control the wafer temperature. The accuracy of the temperature was within 5 °C . A shematic diagram of the experimental setup is shown in Fig.1. Typical temperature-time profiles are shown in Fig.2. Good linearity was obtained in the temperature range of 400-1000 °C for various ramp-up rates. RTO oxidation was performed as follows: first, the temperature was raised from 400°C to the desired temperature (RTO temperature) at a constant ramp-up rate, then this temperature was held for the desired time (RTO time), and then oxidation was ended by switching off the lamp. During this sequence, oxygen gas flowed continuously and its flow rate was fixed at 1 ℓ /min. The oxide film thickness was measured with an ellipsometer with the reflactive index
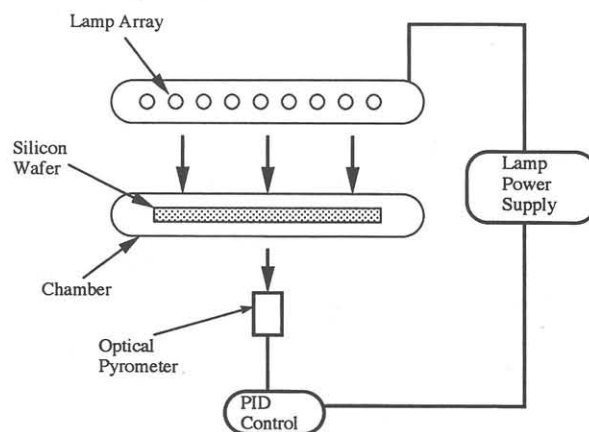


Fig.1 Schematic diagram of the experimental apparatus. Wafer temperature is controlled using a closed system with an optical pyrometer, PID controller and lamp power supply.

Table1. The calculated values, $X_r$, $B/A$, $B$, $E_1$ and $E_2$.

| Temp (℃) | $X_r$ (A) | $B/A$ (A/s) | $B$ (A²/s) | $E_1$ (eV) | $E_2$ (eV) |
|---|---|---|---|---|---|
| 950 | 0.53 | 0.87 | 30.0 | | |
| 1000 | 1.13 | 1.70 | 50.0 | | |
| 1050 | 2.37 | 3.30 | 92.0 | 2.00 | 1.74 |
| 1100 | 4.49 | 34.5 | 200.0 | | |
| 1150 | 9.14 | 12.8 | 350.0 | | |
| 1200 | 17.8 | 20.0 | 700.0 | | |

at 1.460. The oxide thickness was evaluated after averaging five measurements within an area of 4-inch diameter around the center of the wafer. The uniformity of the oxide in the area was better than 1% per sigma.

## 3. RESULTS & DISCUSSION

Fugure 3 illustrates the relationship between the oxide thickness and the oxidation time for various oxidation temperatures. For the oxidation below 1000 ℃, the growth rate is fairly small, and the maximum oxide thickness seems to be limited to 5 nm. With increasing oxidation temperature, the oxide thickness increases. For 1200 ℃, the thickness becomes greater than 20 nm. Moreover, the initial oxide thickness seems to increase from 1 to 4 nm with increasing oxidation temperature.

An attempt was made to obtain the best possible fit to the RTO growth curve. For the analysis, the linear-parabolic low[8] proposed by Deal and Grove was used to represent the growth curve. This postulate is based on the fact that by irradiating with light, heat transfer occurs via phonon emission and diffusion in the RTO process. As seen in Fig.3, initial thickness is strongly dependent on the RTO temperature. It is important to note that the oxide growth at ramp-up must be taken into consideration, because the wafer is usually in oxygen atmosphere even at the ramp-up stage. To estimate the oxide increase at the ramp-up stage, the temperature profile is reproduced by the sum of the step functions, as shown in Fig.4. In this case, the time and temperature at each step are defined as, $t_i = (t_r/n)x_i$, $T_i = \alpha t_i + T_0$ ($i = 0, 1, 2, \cdots, n$), $T_r = T_{max} - T_0$, where $\alpha$ is the ramp-up rate (=100℃/s), $T_0$ is the starting temperature (=400℃), and $T_{max}$ is the RTO temperature desired. We calculate the initial oxide increase ($X_r$) using these equations. If $X_r$ is small, reaction-limited oxidation is dominant in the ramp-up stage: in fact, $X_r$ is considered to be within 3 nm. Thus, $X_r$ can be expressed as, $X_r = \sum C_1 \Delta t \exp[E_1/k(\alpha t_i + T_i)]$, where $C_1$ is the constant which is determined by the oxidant concentration and substrate orientation, $E_1$ is activation energy. If the reaction is always realized to the limit of $\Delta t \to 0$, this equation approaches the integrated form. From this equation, oxide thickness $X$ is expressed as,

$$X(t) = \{-A + \sqrt{A^2 + 4[(X_0 + X_r)^2 + A(X_0 + X_r)] + Bt}\}/2,$$

where $A$ and $B$ are the constants, which are derived from the linear rate constant $B/A$ and parabolic rate constant $B$, $X_0$ is the oxide thickness at $t = 0$. With the use of this equation,
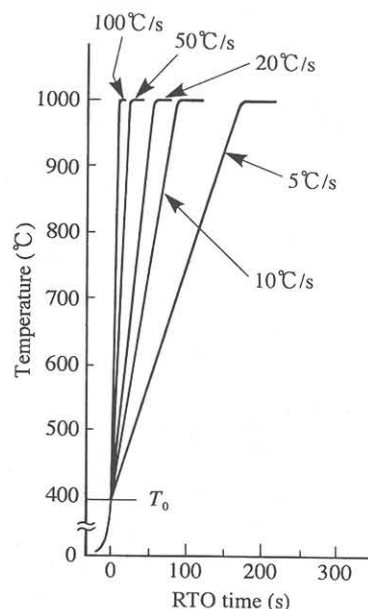


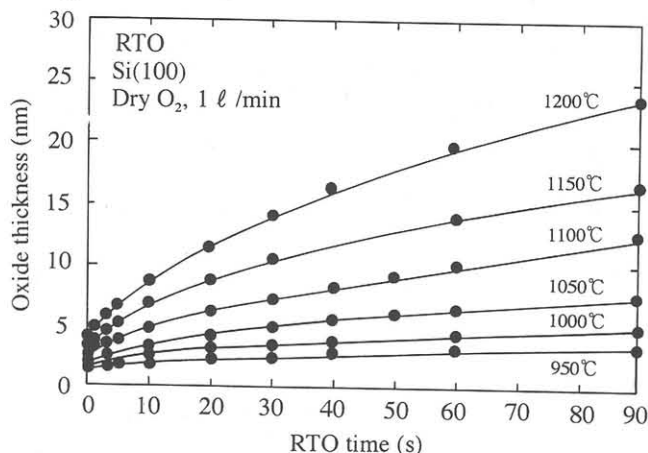Fig.2  Typical temperature-time profiles in ramp-up condition for the ramp-up rates in the range of 5-100℃/s.



Fig.3  Relationship of oxide thickness and oxidation temperatures. The ramp-up rate was fixed at 100℃/s. The lines are calculated for the linear-parabolic law in the text.

the calculated curves are well fitted to the experimental data. Table 1 shows the calculated values, $X_r$, $B/A$ and $B$. The initial growth enhancement can be fully explained by the oxide increase under ramp-up condition.

Figure 5 shows the Arrhenius plot for the $B/A$ and $B$. The activation energies evaluated in curve fitting are $E_1 = 2.00$ eV for $B/A$ and $E_2 = 1.74$ eV for $B$, respectively. The activation energy $E_1$ is in rather good agreement with the value for dry furnace oxidation reported Deal
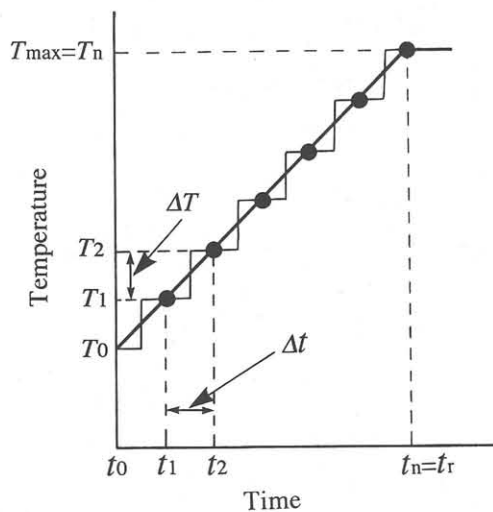
Fig.4 The step functions reveal the temperature profile in ramp-up conditions. The $t$ and the $T$ are the time and the temperature intervals, which are defined as $\Delta t = t_{i+1} - t_i$, $\Delta T = T_{i+1} - T_i$.
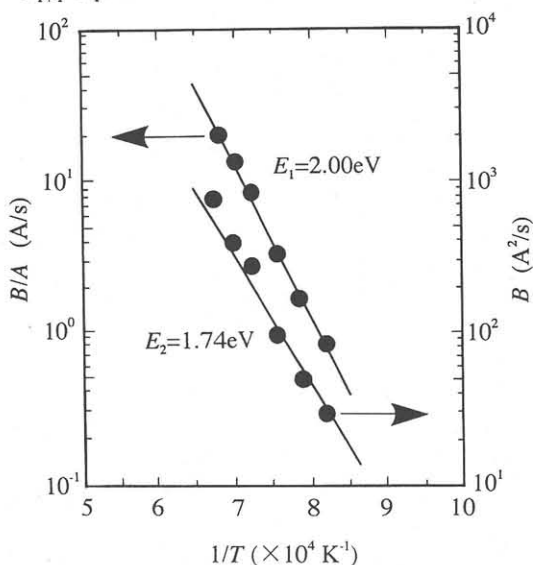


Fig.5 Arrhenius plot for the linear rate constant $(B/A)$ and the parabolic rate constant $(B)$. The activation energies are calculated to be $E_1 = 2.00$ eV and $E_2 = 1.74$ eV.
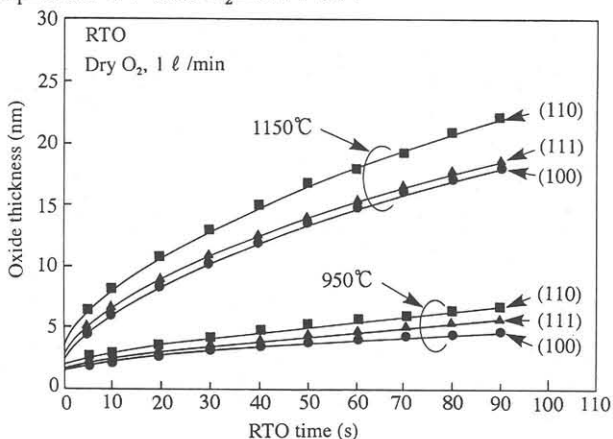


Fig.6 Oxide thickness versus oxidation time for Si(100), (111) and (110). The oxide growth rate increases in the order: (100), (111) and (110).

and Grove. The $B/A$ is dominated by the reaction at the $SiO_2/Si$ interface. This $E_1$ value is in close agreement with the energy required to break Si-Si bonds, which is 1.83 eV/molecule. For RTO oxidation, the $E_2$ value is 1.74 eV, which is larger than the case of dry furnace oxidation (1.23 eV). This means that a large diffusivity of oxygen is realized in RTO kinetics. However, the reason of this mechanism is still unknown. Orientation dependence in RTO kinetics is shown in Fig.6. The growth rate increases in the order: (100), (111) and (110). This behavior is explained by the atom concentration on the silicon surface. The growth rate of (110) is larger than that of (100) [(110):(100)=1.42:1]. This is originated from the difference of the atom density of two-dimensional plane.[9] This orientation dependence effect can be also reproduced using our model in which the values, $B/A$ and $B$ are well chosen.

## 4. CONCLUSION

A practical model for rapid thermal oxidation (RTO) has been proposed for the first time. Good agreement with experimental data has been achieved using the linear-parabolic law proposed by Deal and Grove. In this model, oxide growth at the ramp-up state in the RTO process is fully taken in account. In our model, the initial growth enhancement can be well expressed by including the reaction-limited oxidation in the Deal-Grove model. The results showed that the activation energies for the linear rate constant $B/A$ and fro the parabolic rate constant $B$ are 2.00 eV and 1.74 eV, respectively. In conclusion, the overall growth mechanism of the RTO kinetics is almost the same as in dry furnace oxidation, and can be descrived with initial growth enhancement in the ramp-up condition.

## REFERENCES
1) J.R.Brews, W.Fichtner, E.H.Nicollian and S.M.Sze, IEEE Electron Device Lett. **EDL-1** (1980) 2.
2) A.M.Goodman and J.M.Breece, J.Electrochem.Soc. **117** (1970) 987.
3) Y.Kamigaki and Y.Ito, J.Appl.Phys.**48** (1979)1573.
4) R.R.Razouk and B.E.Deal, J.Electrochem.Soc. **126** (1979) 1573.
5) J.Nulman, J.P.Krusius and A.Gat, IEEE Electron Device Lett. **EDL-6** (1985) 205.
6) H.Fukuda,T.Iwabuchi and S.Ohno, Jpn.J.Appl.Phys. **27** (1988) L2164.
7) R.B.Fair, *Rapid Thermal Processing* (Academic Press, New York, 1993) 45.
8) B.E.Deal and A.S.Grove, J.Appl.Phys. **36** (1965) 3770.
9) E.H.Nicollian and J.R.Brews, *MOS (Metal Oxide Semiconductor) Physics and Technology* (John Wiley & Sons, New York, 1982) 686.